Three-dimensional wind profiling of offshore wind energy areas with airborne Doppler lidar

Grady J. Koch
Jeffrey Y. Beyon
Larry J. Cowen
Michael J. Kavaya
Michael S. Grant

Three-dimensional wind profiling of offshore wind energy areas with airborne Doppler lidar

Grady J. Koch,* **Jeffrey Y. Beyon, Larry J. Cowen, Michael J. Kavaya, and Michael S. Grant**
NASA Langley Research Center, Hampton, Virginia 23681

Abstract. A technique has been developed for imaging the wind field over offshore areas being considered for wind farming. This is accomplished with an eye-safe 2-μm wavelength coherent Doppler lidar installed in an aircraft. By raster scanning the aircraft over the wind energy area (WEA), a three-dimensional map of the wind vector can be made. This technique was evaluated in 11 flights over the Virginia and Maryland offshore WEAs. Heights above the ocean surface planned for wind turbines are shown to be within the marine boundary layer, and the wind vector is seen to show variation across the geographical area of interest at turbine heights. © *The Authors. Published by SPIE under a Creative Commons Attribution 3.0 Unported License. Distribution or reproduction of this work in whole or in part requires full attribution of the original publication, including its DOI.* [DOI: 10.1117/1.JRS.8.083662]

1 Introduction

Wind over oceans and the Great Lakes provides a potentially rich source of renewable energy. An advantage of offshore wind over land-based wind farms is that the wind over oceans and large lakes is typically strong and steady. On the other hand, offshore wind farms are more difficult to develop in the complexities of engineering structures in a marine environment. For example, the typical terrestrial approach of evaluating the wind at a site with a meteorological tower equipped with anemometers is extremely expensive to implement in the offshore environment. Remote sensing of wind offers an attractive alternative to meteorological towers, and several designs have been used involving Doppler lidars mounted on bouys, platforms, or ships.[1–5] These lidar implementations (as well as a meteorological tower) only measure the wind over a point, though. Offshore wind energy areas (WEAs) can be of such a large size (27.8 by 22.2 km for the Virginia offshore WEA) that using one or a few point measurements may not offer sufficient representation of the wind resource. The implementation described here demonstrates a means to image the wind over a volume of a WEA by rapidly moving a downward-looking lidar through the area from onboard an aircraft.

2 Lidar Instrument Design

The lidar used, called the Doppler aerosol wind lidar (DAWN), has been used previously in several ground-based applications.[6–8] More recent work has engineered the instrument into a flight-capable form. The DAWN's first flights were in 2010 aboard the NASA DC-8 (4 engine jet) aircraft to support the Genesis and Rapid Intensification Processes hurricane study.[9,10] Follow-on flights were made with the instrument installed on the UC-12B (2 engine turboprop) aircraft shown in Fig. 1, including the research described here.

A summary of DAWN's specifications is given in Table 1. The heart of the lidar instrument is a Ho:Tm:LuLiF-pulsed laser and single-pass amplifier.[11] A single-frequency output is obtained

*Address all correspondence to: Grady J. Koch, E-mail: grady.j.koch@nasa.gov

Fig. 1 The Beechcraft Huron UC-12B aircraft.

by injection seeding the pulsed laser with a continuous-wave Ho:Tm:YLF laser. Part of the injection seed laser is also used as a local oscillator for heterodyne detection in the receiver. The output laser beam is spatially expanded by a Dall-Kirkham telescope before passing through a silicon wedge. This wedge deflects the beam in elevation by 30 deg from nadir. By rotating the silicon wedge with a ring motor, the lidar beam can be steered in azimuth to view multiple line of sight Doppler observations with which to compose a horizontal vector wind measurement. Atmospheric backscatter returns into the lidar on the same telescope used for outgoing laser beam expansion; the transmitted and received beams are separated by polarization. Heterodyne mixing of the atmospheric backscatter and local oscillator with InGaAs photodiodes results in an electronic signal which is digitized at 500 Ms/s.

The laser and optical components (except for the beam scanning wedge) are held within a cylindrical enclosure, shown in Fig. 2, that is mounted over a window in the belly of the aircraft. The enclosure is attached to the aircraft seat tracks via a structure to facilitate beam alignment to the aircraft window and isolate aircraft vibration from affecting laser performance. The silicon scanning wedge is mounted directly above the aircraft window to allow space for the 30-deg deflected beam to pass unblocked through the aircraft window. Aside from the laser/optical enclosure, three 19-inch racks of equipment are mounted inside the aircraft for water cooling

Table 1 Specifications of lidar. This listed range and velocity resolutions are for real-time computation and display.[8] Later processing and analysis can be at any desired altitude setting with adjustable range-bin size and Fourier transform zero padding.

Parameter	Value
Laser material	Ho:Tm:LuLiF
Pulse energy	250 mJ
Pulse width	200 ns
Pulse repetition rate	10 Hz
Spectrum	Single frequency
Wavelength	2053.5 nm
Beam quality (M_2)	<1.3 times diffraction limit
Detector	InGaAs in dual-balanced configuration
Telescope aperture	15 cm
Scanner	17-cm diameter rotating silicon wedge with 30 deg from nadir deflection angle
Signal processing	500 Ms/s, 10-bits, real-time computation
Range resolution	153-m, overlapped 50% for real-time computation
Velocity resolution	1-m/s line of sight for realtime computation

Fig. 2 The Doppler aerosol wind lidar instrument installed inside the UC-12B aircraft. A cylindrical enclosure houses the laser and and optical receiver.

of the laser, control of laser functions, navigation sensing, and signal processing. Real-time wind measurements are displayed for an operator seated at a 19-inch rack.

A key feature in operation from the aircraft is in compensation of aircraft motion.[12] The forward motion of the aircraft creates a platform-induced Doppler shift that can be much higher than the wind Doppler shift to be measured. In addition, the aircraft's roll, pitch, and yaw create a constantly varying deviation in the angles involved. Our approach to removing the effects of aircraft motion involves attaching a navigation sensor (an inertial navigation system/global positioning system unit) to the lidar instrument to measure aircraft motion. An algorithm was developed to decompose aircraft motion vectors into an aircraft-centric coordinate system to which the lidar beam scanning angles are oriented. Once the aircraft-induced Doppler shift is known along each scan angle, it is subtracted from the measured total Doppler shift to find the wind-induced Doppler shift. Multiple line-of-sight Doppler shifts can then be combined to find the wind vector in an aircraft-centric coordinate system. The wind vector is then placed into the desired true-north coordinate system based on the measured direction of the aircraft's heading. Using the backscatter from the ground serves as a check on the efficacy of aircraft motion compensation technique. That is, since the ground is not moving with the wind, the Doppler shift measured from the ground backscatter should match the motion of the aircraft. Analyzing these ground backscatter returns shows that all aircraft motion effects (and the means by which they are measured) are compensated for to <1 m/s.

The design for scanning the lidar beam allows sweeping the beam to any desired azimuth. In the measurements described here, two orthogonal azimuths are used set at 45 deg to either side of a forward-looking line along the length of the aircraft. The line-of-sight Doppler shift along these two azimuths forms components to sum to find the horizontal wind vector. Compared with many-axis velocity-azimuth type scans, this two-axis approach has the advantage of allowing rapid measurement, but the disadvantage of requiring the assumption that the vertical component of wind is zero. The wind energy application has a stronger need for rapidly updated horizontal wind profiling than for vertical wind component determination. In the measurements that follow, a wind profile was made every 15 s from 60-pulses viewed at each of the orthogonal azimuths.

The DAWN wind measurement results have been validated against a several other sensors. With DAWN operating from the ground comparisons showing accurate results have been made

against anemometers, balloonsondes, and other wind lidars.[6,13,14] Airborne results from DAWN have been checked against dropsondes and flights over a ground-based 915-MHz radar profiler.[9]

3 Measurement Approach

Our desire was to measure the wind throughout a volume over an offshore WEA. A stationary lidar finds a profile of wind with altitude, and by moving the lidar over the area of interest profiles can be made throughout a volume. In other words, we used the aircraft to raster scan the WEA. We probed two WEAs identified by the United States Bureau of Ocean Energy Management (BOEM): off shore of Virginia Beach, Virginia and off shore of Ocean City, Maryland. Notional aircraft flight paths overlaid with BOEM maps of these WEAs are shown in Figs. 3 and 4. The flight crew of the UC-12B was able to closely match the notional flight path, with an example actual flight path shown in Fig. 5 of a mission to probe the Virginia WEA. The WEAs were sampled in 12 east-west "transits," separated from each other in the north–south direction by 1.2 km for the Virginia WEA and 2.2 km for the Maryland WEA.

Fig. 3 Map of the Virginia offshore wind energy area (WEA). The WEA is composed of 20 outer continental shelf blocks, shaded white in this map. Red shaded areas are warning areas of restricted air space. The notional aircraft flight path is drawn as a blue line.

Fig. 4 Map of the Maryland offshore WEA. The WEA has areas in 19 outer continental shelf blocks, shaded green in this map. Twelve east–west transits are made over the WEA, drawn as blue lines.
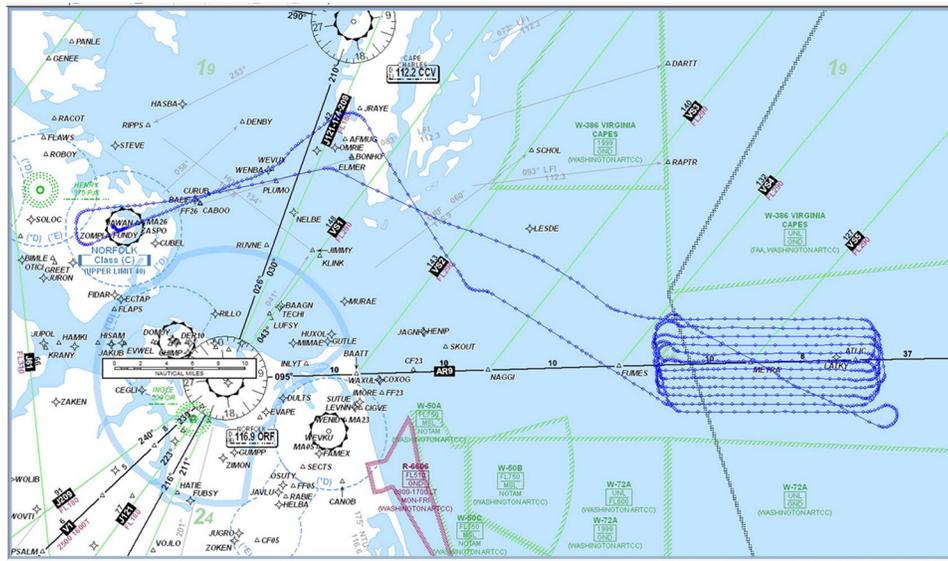
Fig. 5 Aircraft actual flight path (blue line) to probe the Virginia WEA. The aircraft took off from Langley Air Force Base in Hampton, Virginia.

A total of 11 flight tests, summarized in Table 2, were made on different days in a campaign in 2012 and another in 2013. The lidar configuration was the same between the 2012 and 2013 flight campaigns, except for some technology improvements for the 2013 flights. These improvements included a change in the laser temperature operating point after learning from the 2012 flights on the UC-12B that the aircraft cabin interior tends to get warm. Also, the beam expanding telescope was refurbished for the 2013 flights after finding laser-induced damage to the telescope's secondary mirror. The altitude at which to fly was

Table 2 Summary of flight tests.

Date	Time (local) period of flight over wind energy area (WEA)	WEA area	Comments
November 1, 2012	10:14 to 11:20	Virginia	Full coverage of WEA
November 2, 2012	9:39 to 11:07	Virginia	Full coverage of WEA
November 6, 2012	9:23 to 10:33	Virginia	Partial coverage due to laser problem with cabin temperature
November 16, 2012	2:56 to 14:36	Virginia	Aircraft went to low altitude to get under thick cloud cover
November 28, 2012	13:10 to 15:00	Virginia	Partial coverage due to laser problem with cabin temperature
June 14, 2013	10:45 to 11:47	Virginia	Full coverage of WEA despite clouds
June 21, 2013	9:40 to 10:49	Virginia	Partial coverage due to very thick overcast
June 24, 2013	12:34 to 13:42	Maryland	Full coverage of WEA
June 26, 2013	12:13 to 13:23	Maryland	Full coverage of WEA
June 28, 2013	9:15 to 10:52	Virginia	Full coverage of WEA
July 10, 2013	9:10 to 10:15	Virginia	Full coverage of WEA despite clouds

selected considering several factors: keeping the scanned beam area small over the ocean surface, avoiding interference from clouds, a desire to reach the primary target heights of ocean surface to 200 m, and air traffic control issues. The scanned beam area is considered because the 30-deg deflection from nadir involved with the silicon wedge, along with the ±45-deg azimuth scan used to view two components of the wind, means that the area scanned over the ocean increases with aircraft altitude. An assumption in the wind measurement technique is that the wind is uniform over the area scanned, and if this area becomes too large the assumption of uniform wind may become problematic. In order to keep the scanned area reasonably small, we chose an aircraft altitude of 1.5 km as an upper limit. At an aircraft altitude of 1.5 km, the scanned beam area at the ocean surface has a radius of 750 m due to the 30 deg from nadir wedge deflection angle. An assumption of wind being constant over this circular area of 1.5 km is on the same order of the distance traversed by the aircraft during one scan pattern. At 135-m/s airspeed typical of the UC-12B, the aircraft travels 2 km during the 15 s required to scan for one wind profile. Flying at 1.5-km altitude, aside from creating a reasonably sized scan area near the ocean surface, has a benefit of profiling the wind well above the marine boundary layer to provide a detailed meteorological picture. To summarize the scan pattern used for this work, two line-of-sight Doppler shift measurements (made at ±45-degrees azimuth from a line looking forward of the long axis of the aircraft) are combined to determine the horizontal wind vector. Each line of sight is viewed for 6 s for an averaging of 60 laser pulses. With time needed to turn the beam scanner, a wind profile is thus made every 15 s. With the forward motion of the aircraft, 15 s per profile creates a data point every 2 km in the horizontal direction.

Although the wind data above the marine boundary layer is useful for meteorological studies, the altitude of most interest is that of potential turbine heights to 200-m above the ocean surface. If clouds are in the area over the WEA, then it may become desirable to fly lower for a clear path of the lidar beam to the primary target of 0 to 200-m altitude. The laser pulse energy, being a rather strong output, has some capability for working through clouds. With this ability, a guideline was derived based on cloud cover encountered as the aircraft arrives at the WEA. Taking aviation definitions of cloud cover, if cloud conditions are none, few, or scattered then a flight altitude of 1.5 km is maintained. If cloud conditions are broken to overcast at 1.5 km, then the pilot descends the aircraft to try to get under the thick clouds. If broken to overcast conditions persist down 600-m altitude, then the aircraft is held at 600-m.

For both the Virginia and Maryland WEAs, the area was sectioned into 12 east-to-west transits. Including aircraft turns to line up the various transits, a scan of a WEA takes about 70 min to complete. With a typical speed of the aircraft at 135-m/s and a scan time of 15 s, a wind profile is made at an interval of ~2 km. Video 1 shows the view from the lidar operator's perspective, panning around from over the pilot's shoulder to a view out the window. This video was made on November 16, 2012, when thick clouds forced the aircraft to 600-m altitude.

Video 1 View from inside aircraft during flight over Virginia WEA (MP4, 1.35 MB) [URL: http://dx .doi.org/10.1117/1.JARS.8.1.083662.1].

4 Wind Mapping: Horizontal Slicing

With profiles resolved in altitude from the moving aircraft, the wind at a particular altitude can be mapped over the entire WEA. An example such map at 100-m above the ocean surface of the Virginia WEA is shown in Fig. 6. A smoothing color-encoding algorithm is used to represent contours of the wind vector. A height of 100-m was selected to match a typical size of an offshore turbine, with hub height of 100 and 50-m-long blades.

A significant amount of variation and structure is seen in the wind vector of Fig. 6, with values observed between 7 to 18 m/s in speed and 250 to 320 deg in direction. A spatial trend can be seen in the wind vector of this particular example as speed increasing with distance east and south, and direction rotating clockwise with distance north. Several factors may be coming into play to create this spatial structure. First, the 100-m height is within the atmospheric boundary layer where wind flow can be turbulent. Creating the same plot at 600-m height, which is above the boundary layer, shows a more uniform wind field. The interface between the atmospheric boundary layer and free troposphere can be determined by viewing vertical slices of the WEA, the subject of the following section. Second, offshore WEAs are close enough to shore to be affected by the sea breeze.[15,16] Third, the eastern edge of the Virginia WEA is close enough to the Gulf Stream that wind may be influenced by differences in ocean water temperature.[16] The other eight flight tests over the Virginia WEA made in 2012 and 2013 showed similar spatial variations and trends of the wind vector, though the east–west, north–south trends varied. The lowest and highest wind speeds observed at 100-m height over all the flights were 2 and 20 m/s, respectively. Wind maps at different altitudes of interest can be made, as shown in Fig. 7 at 50 and 150-m above the ocean surface for the same data set of Fig. 6 over the Virginia WEA. These two altitudes were chosen as they represent the bottom and top of a blade span for a possible offshore wind turbine. With this view over a blade span, wind shear can be determined that could create a torqueing force on the turbine. Inspecting the wind speed at the two heights of Fig. 7 shows that wind is in general higher at 150-m height than 50 m. Some areas of the WEA show a difference in wind speed as much as 4 m/s of a supposed 100-m-long blade span.
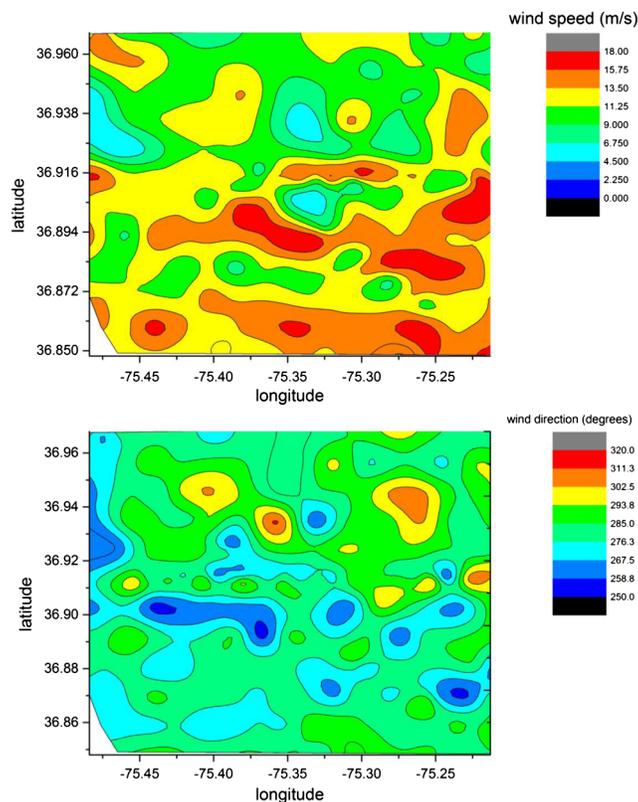

Fig. 6 Map of wind vector at 100-m above ocean surface of Virginia WEA measured on November 2, 2012.
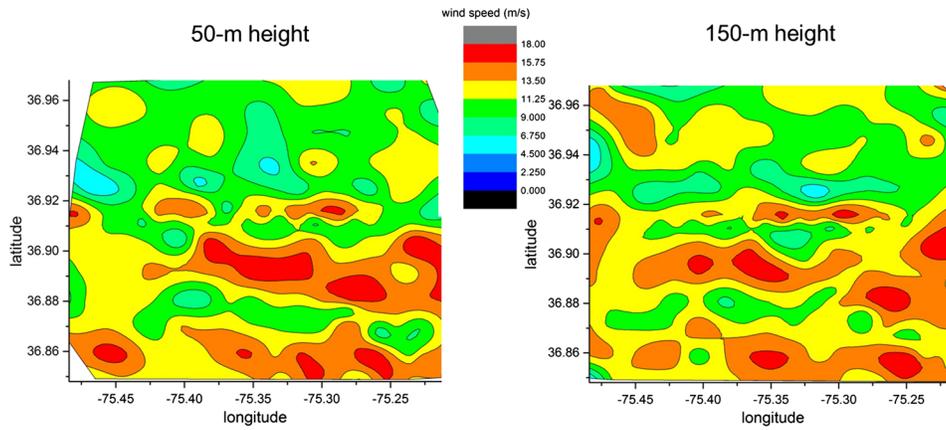
Fig. 7 Maps of wind speed over Virginia WEA at heights corresponding to top and bottom of a turbine blade span.
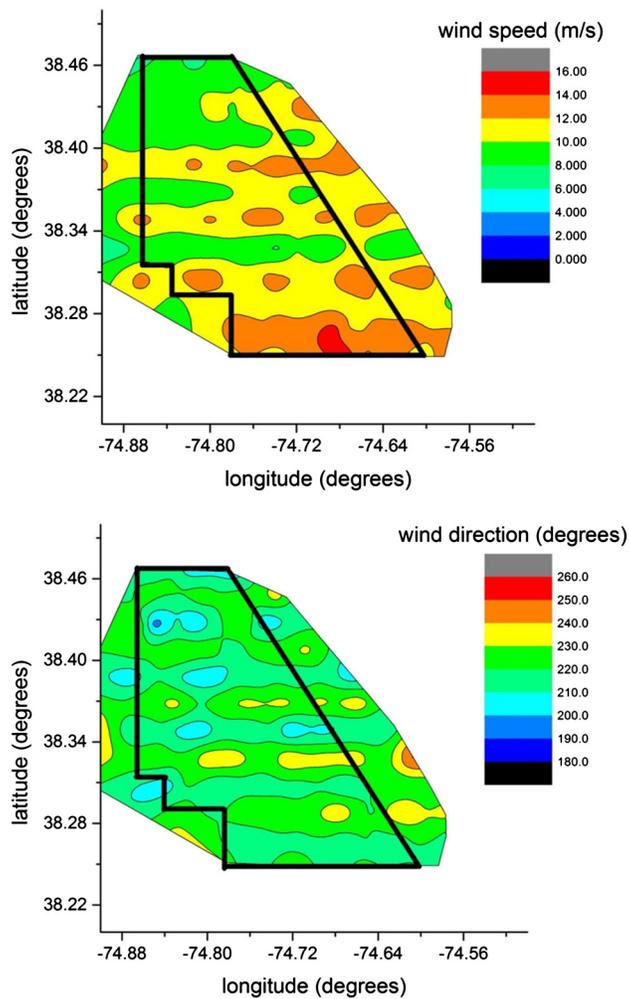

Fig. 8 Map of wind vector at 100-m above ocean surface of the Maryland WEA measured on June 24, 2013.
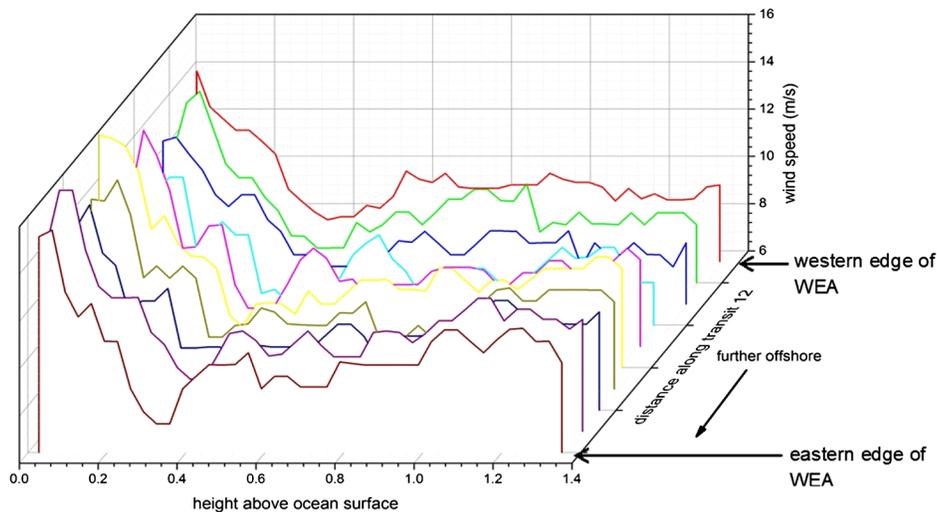
Fig. 9 Vertical slice of wind profiles through southern-most (transit 12 of Fig. 4) boundary of Maryland WEA.

Flights were also made of the Maryland WEA near Ocean City, with the aircraft using Hampton, Virginia as a home base without a need to refuel the aircraft. A wind map for 100-m height, processed in the same way as Fig. 6, is shown in Fig. 8. The Maryland WEA has an irregular shape compared with the Virginia WEA, requiring a somewhat more complicated aircraft path. Significant variation in the wind vector is seen in the Maryland example, with speed varying between 8 and 16-m/s across the WEA.

5 Wind Mapping: Vertical Slicing

Although the previous section displayed horizontal sheets of wind measurements at a fixed altitude, further structure of the wind field is seen by taking vertical slices along a fixed horizontal line of aircraft motion. Figure 9 shows such a vertical slice taken along the southern boundary of the Maryland WEA. This boundary is labeled as "transit 12" in Fig. 4. Along this east–west line of travel, the lidar made 10 profiles. These profiles reveal a boundary-layer effect with a layer of decreasing wind from the ocean surface to 300 to 400-m height and a more uniform wind field above. As distance increases from shore the near-surface layer gets shallower in depth. Turbines would be operating in this marine boundary layer, which the lidar's vertical slicing shows to be spatially varying across the WEA. Much of the spatial structure seen at constant altitudes (Figs. 6–8) is likely related to marine boundary layer variations.

6 Conclusion

An airborne Doppler lidar can provide detailed information of the wind vector over offshore WEAs. For wind energy applications, this technique allows a snapshot view of the wind vector over the large geographical extent of offshore WEAs. An airborne lidar offers a new means to determine both horizontal and vertical spatial trends in the wind vector, which a stationary sensor cannot provide. One possible use of this new capability is as truth data for meteorological models of the wind vector in order to test and improve model performance. For example, if a model's predications are thought to be inaccurate in particular conditions (such as during the diurnal transition of the sea breeze direction) then the airborne lidar could be sent to measure the wind vector in these conditions. Although the airborne lidar wind measurements do provide quick volumetric scans of a wind field, it is not suited to long time scale and long-term averaging that are of interest to many aspects of wind energy production. It is technically feasible, though probably prohibitively expensive, to deploy the lidar on a drone aircraft such as the Global Hawk for continuous scans of a WEA. Instead, the airborne lidar would likely be better used in

conjunction with long term, stationary sensors such as upward-looking lidars on buoys. Given the large geographic areas of offshore WEAs, satisfactorily representing the WEA with buoy-based sensors may require a large number of sensors, or fewer buoys moved from place to place over a longer time span. For example, for the geography of the Virginia WEA and the variations seen by the high-spatial sampling of the airborne lidar, a four by four grid of buoy-based sensors (a total of 16 simultaneously running buoys) would be needed as a minimum to capture the relevant spatial variations in wind. A more cost effective arrangement may be to deploy a few buoy sensors for long-term measurements complemented with occasional airborne lidar scans to build confidence in interpolating or extrapolating the few stationary sensors to represent the entire WEA. Another potential application of airborne lidar is for rapid delivery of wind measurements if, for example, preliminary assessment is being made of an area's wind resources. This rapid delivery is allowed in that overflying an area takes little in approval or permitting procedures compared with installation of an ocean platform or buoy.

By using a high-energy Doppler lidar, wind vectors from an aircraft altitude of 600 m to the ocean surface could be made to reveal the structure of the marine boundary layer and free troposphere, even in conditions of scattered cloud conditions. Eleven flight tests showed significant structure of the wind vector at likely turbine heights throughout the area of WEAs being considered. Understanding of this structure is likely to be economically relevant to wind farm development. Aerosol backscatter conditions encountered in the oceanic environment were often at a low level, such that a lower energy lidar would possibly have difficulty making wind measurements or have to fly at a lower altitude in order to make measurements in the critical altitude range of 100 to 200 m.

Acknowledgments

References

1. A. Peña et al., "Offshore wind profiling using light detection and ranging measurements," *Wind Energy* **12**(2), 105–124 (2009), http://dx.doi.org/10.1001/we.283.
2. A. Rettenmeier et al., "Development of LiDAR measurements for the German offshore test site," *IOP Conf. Ser.: Earth Environ. Sci.* **1**, 012063 (2008), http://dx.doi.org/10.1088/1755-1315/1/1/012063.
3. Y. L. Pichugina et al., "Doppler Lidar-based wind-profile measurement system for offshore wind-energy and other marine boundary layer applications," *J. Appl. Meteorol. Climatol.* **51**(2), 327–349 (2012), http://dx.doi.org/10.1175/JAMC-D-11-040.1.
4. S. Hannon et al., "Large scale wind resource mapping using a state of the art 3D scanning lidar," in *Am. Wind Energy Assoc. (AWEA) WINDPOWER 2008 Conf.*, Houston, Texas (2008).
5. Y. Käsler, S. Rahm, and R. Simmet, "Wake measurements of a multi-MW wind turbine with coherent long-range pulsed Doppler wind lidar," *J. Atmos. Oceanic Technol.* **27**(9), 1529–1532 (2010), http://dx.doi.org/10.1175/2010JTECHA1483.1.
6. G. J. Koch et al., "Side-scan Doppler lidar for offshore wind energy applications," *J. Appl. Remote Sens.* **6**(1), 063552 (2012), http://dx.doi.org/10.1117/1.JRS.6.063562.
7. G. J. Koch et al., "Field testing of a high-energy 2-μm Doppler lidar," *J. Appl. Remote Sens.* **4**(1), 043512 (2010), http://dx.doi.org/10.1117/1.3368726.

8. G. J. Koch et al., "High-energy 2-μm Doppler lidar for wind measurements," *Opt. Eng.* **46**(11), 116201 (2007), http://dx.doi.org/10.1117/1.2802584.

9. M. J. Kavaya et al., "The Doppler aerosol wind lidar (DAWN) airborne, wind-profiling, coherent-detection lidar system: overview, flight results, and plans," *J. Atmos. Oceanic Technol.*, 00274.1, in press (2013), http://dx.doi.org/10.1175/JTECH-D-12-00274.1.

10. S. Braun et al., "NASA's genesis and rapid intensification processes (GRIP) field experiment—bringing new technologies to the hurricane intensity problem," *Bull. Am. Meteorol. Soc.* **94**(3), 345–363 (2013), http://dx.doi.org/10.1175/BAMS-D-11-00232.1.

11. J. Yu et al., "1 J/pulse Q-switched 2-μm solid state laser," *Opt. Lett.* **31**(4), 462–464 (2006), http://dx.doi.org/10.1364/OL.31.000462.

12. J. Y. Beyon et al., "Airborne wind profiling algorithms for the pulsed 2-micron coherent Doppler lidar at NASA Langley Research Center," *Proc. SPIE* **8731**, 87310K (2013), http://dx.doi.org/10.1117/12.2015952.

13. G. D. Emmitt, S. A. Wood, and G. Koch, "Comparison of GWOLF and VALIDAR Doppler Lidar measurements," in *American Meteorological Society 2nd Symp. Lidar Atmos. Appl.* (2005).

14. K. C. Vermeesch et al., "A review of wind comparison work at the Howard University Beltsville Research Campus," in *American Meteorological Society 6th Symp. Lidar Atmos. Appl.* (2013).

15. J. E. Simpson, *Sea Breeze and Local Wind*, The University Press, Cambridge, UK (1994).

16. C. J. Steele et al., "Idealized WRF model sensitivity simulations of sea breeze types and their effects on offshore windfields," *Atmos. Chem. Phys.* **13**, 443–461 (2013), http://dx.doi.org/10.5194/acp-13-443-2013.

Grady J. Koch received his BS in electrical engineering in 1991 from Virginia Tech, an MS in electrical engineering in 1995 from the University of Illinois at Urbana-Champaign, and his PhD in electrical engineering in 2001 from Old Dominion University. In 1987, he began work at NASA Langley Research Center as a cooperative education student, taking regular employment there in 1991. His research interests include coherent lidar, differential absorption lidar, solid-state lasers, and diode lasers.

Jeffrey Y. Beyon received his BS from Kyung Hee University, Korea (1989), an MS from the University of Wisconsin, Madison (1992), and his PhD from the Pennsylvania State University, University Park (1997), all in electrical engineering. His research is centered on high-speed data acquisition system and software design, lidar signal processing algorithm development, and statistical signal processing. He has been working with NASA Langley Research Center in Virginia since 2001 on numerous projects.

Larry J. Cowen is a graduate of the NASA Langley Research Apprenticeship program as an electrical engineering technician and is a member of the Certified Aerospace Technician Core (SpaceTEC). He has been involved in the development of earth science projects flown on the space shuttle as well as NASA aircraft since 1987. He is currently a quality assurance aerospace specialist for various projects throughout Langley Research Center.

Michael J. Kavaya has worked on coherent-detection pulsed lidar for over 30 years. He received his PhD in EE from Caltech and then began his career at NASA/JPL with a CO_2 coherent lidar studying aerosol backscatter. He then joined Coherent Technologies, Inc. and developed the first solid-state coherent Doppler wind lidar at 1 μm, and then the first eyesafe version at 2 μm. He then joined NASA to work on measuring winds from space.

Michael S. Grant is an electrical engineer at the NASA-Langley Research Center, Hampton, Virginia, where he has worked in the areas of spaceflight electronics design, systems engineering, and signal processing on a number of space shuttle, aircraft-based, and satellite-based atmospheric science projects. His electrical engineering degrees are the BS from Old Dominion University in 1986, the ME from the University of Virginia in 2001, and the PhD from the University of Virginia in 2006. His research interests include Earth remote sensing, image processing, and pattern classification.